

Integrated superconducting circuit for qubit and resonator protection

Xiao-Pei Yang(杨晓沛), Zhi-Kun Han(韩志坤), Shu-Qing Song(宋树清), Wen Zheng(郑文), Dong Lan(兰栋), Xin-Sheng Tan(谭新生), and Yang Yu(于扬)

Citation: Chin. Phys. B, 2021, 30 (**7**): 078403. DOI: 10.1088/1674-1056/ac003d
Journal homepage: http://cpb.iphy.ac.cn; http://iopscience.iop.org/cpb

What follows is a list of articles you may be interested in

Stretchable electromagnetic interference shielding and antenna for wireless strain sensing by anisotropic micron-steel-wire based conductive elastomers

Xiaoyu Hu(胡晓宇), Linlin Mou(牟琳琳), and Zunfeng Liu(刘遵峰)
Chin. Phys. B, 2021, 30 (**1**): 018401. DOI: 10.1088/1674-1056/abc2b3

Compact NbN resonators with high kinetic inductance

Xing-Yu Wei(魏兴雨), Jia-Zheng Pan(潘佳政), Ya-Peng Lu(卢亚鹏), Jun-Liang Jiang(江俊良), Zi-Shuo Li(李子硕), Sheng Lu(卢盛), Xue-Cou Tu(涂学凑), Qing-Yuan Zhao(赵清源), Xiao-Qing Jia(贾小氢), Lin Kang(康琳), Jian Chen(陈健), Chun-Hai Cao(曹春海), Hua-Bing Wang(王华兵), Wei-Wei Xu(许伟伟), Guo-Zhu Sun(孙国柱), and Pei-Heng Wu(吴培亨)
Chin. Phys. B, 2020, 29 (**12**): 128401. DOI: 10.1088/1674-1056/abc2b8

The coupling effect of air-bridges on broadband spiral inductors in SiC-based MMIC technology

Jia-Xin Zheng(郑佳欣), Xiao-Hua Ma(马晓华), Yang Lu(卢阳), Bo-Chao Zhao(赵博超), Heng-Shuang Zhang(张恒爽), Meng Zhang(张濛), Li-Xiang Chen(陈丽香), Qing Zhu(朱青), Yue Hao(郝跃)
Chin. Phys. B, 2017, 26 (**8**): 088401. DOI: 10.1088/1674-1056/26/8/088401

Optimal satisfaction degree in energy harvesting cognitive radio networks

Li Zan, Liu Bo-Yang, Si Jiang-Bo, Zhou Fu-Hui
Chin. Phys. B, 2015, 24 (**12**): 128401. DOI: 10.1088/1674-1056/24/12/128401

Study of a millimeter-wave squint indirect holographic algorithm suitable for imaging with large field-of-view

Gao Xiang, Li Chao, Fang Guang-You
Chin. Phys. B, 2014, 23 (**2**): 028401. DOI: 10.1088/1674-1056/23/2/028401

SPECIAL TOPIC — Quantum computation and quantum simulation

Integrated superconducting circuit for qubit and resonator protection*

Xiao-Pei Yang(杨晓沛), Zhi-Kun Han(韩志坤), Shu-Qing Song(宋树清), Wen Zheng(郑文), Dong Lan(兰栋), Xin-Sheng Tan(谭新生), and Yang Yu(于扬)†

National Laboratory of Solid State Microstructures, School of Physics, Nanjing University, Nanjing 210093, *China*

(Received 8 April 2021; revised manuscript received 10 May 2021; accepted manuscript online 12 May 2021)

A semi-infinite waveguide acts as a mirror and helps protect the qubit in front of it from decoherence. Here, we investigate the interference effect in an open waveguide consisting of resonators with different decay rates. We find that a lossy resonator works as a mirror and changes the effective decay rate of the other. The spontaneous radiation of qubit is related to its environment, and we can control it by arranging the lossy resonator's position or frequency. Our approach helps improving the qubit performance, as well as the quantum gate fidelities.

Keywords: interference, decay suppression, Purcell filter

PACS: 84.40.Dc, 12.20.−m, 31.30.J−

DOI: 10.1088/1674-1056/ac003d

1. Introduction

According to the Jaynes–Cummings model, one can obtain the qubit state by the frequency shift of the coupled resonator.[1] This standard dispersive measurement method has been applied to many systems such as superconducting circuits, quantum dots, and cold atoms.[2–5] One may increase the coupling strength between the qubit and the resonator to improve the qubit state distinguishability. However, it comes with more spontaneous emission of the qubit. The decay loss arising from the Purcell effect will reduce the qubit coherence time, degrading the gate fidelity.[6] Improving the qubit decoherence by either reducing the coupling strength or minimizing the resonator decay rate leads to lower discrimination or readout speed. To solve the conflict and enhance the measurement efficiency, researchers proposed techniques based on parametric amplifiers, Purcell filters, and tunable coupling design.[7–12]

Recently, quantum interference between different paths attracts much attention. The constructive (destructive) interference can enhance (suppress) the transmission. Depending on the coupling regime, the electromagnetically induced transparency (EIT) or Fano resonance leads to the symmetric or asymmetric profiles, which has applications in quantum sensing.[13–15] Among these implementation schemes of interferometry, superconducting circuits possess the advantages of integration and design flexibility. It has shown that the interference can protect qubits from decoherence, resulting in an expandable quantum network.[16] However, these interference effects have not been applied to suppress the qubit decay losses via the resonator.

In this paper, we propose an integrated circuit that protects the superconducting resonator or qubit from decoherence. Based on the usual qubit measuring system, we insert a second lossy resonator into the waveguide. The constructive or destructive interference between the resonators decides the effective decay rate of the readout one. The spontaneous emission of qubits is related to its coupled environment. Here we demonstrate how to control it by arranging the second lossy resonator. This scalable design provides a tool to realize noisy intermediate-scale quantum computing.

2. Purcell effect

We show the schematic diagram circuit in Fig. 1. Firstly, we neglect the lossy resonator and consider the Transmon qubit as a two-level system.[17,18] The Hamiltonian of the qubit–resonator interaction system is ($\hbar = 1$)

$$H_{\rm JC} = \omega_{r_1} a_1^\dagger a_1 + \omega_q \frac{\sigma_z}{2} + g(a_1^\dagger \sigma_- + a_1 \sigma_+), \tag{1}$$

where ω_{r_1} is the resonate frequency of the readout resonator, and $a_1^\dagger$ (a_1) is its creation (annihilation) operator. $\sigma_\pm = (\sigma_x \pm {\rm i}\sigma_y)/2$, $\sigma_{x,y,z}$ is the Pauli operator of the qubit. g describes the coupling strength between the readout resonator and qubit.

When $\delta_{r_1,q} = \omega_{r_1} - \omega_q \gg g$, the interaction system is in the dispersive regime.[19] We can obtain the qubit state by the frequency shift of the readout resonator. For example, when the qubit goes from the ground to an excited state, the resonator frequency changes by $2\chi = 2g^2/\delta_{r_1,q}$. The qubit decay

*Project supported by the National Key R&D Progarm of China (Grant No. 2016YFA0301802), the National Natural Science Foundation of China (Grant Nos. 61521001, 12074179, and 11890704), and the Key R&D Program of Guangdong Province, China (Grant No. 2018B030326001).

†Corresponding author. E-mail: yuyang@nju.edu.cn

© 2021 Chinese Physical Society and IOP Publishing Ltd

known as the Purcell effect is $\gamma \approx \kappa_1 g^2/\delta_{r_1,q}^2$.[6] From the expression of χ and γ, we find that a larger $\delta_{r_1,q}$ corresponds to a lower qubit decay loss. However, this method reduces the measurement sensitivity. To solve this problem, we can insert a lossy resonator between the readout one and the waveguide. It is known as the Purcell filter,[8–10] which changes the qubit coupled environment and isolates the qubit from decoherence channels.

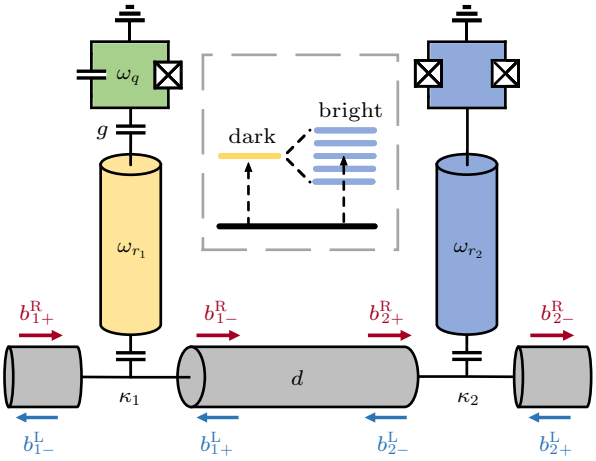


Fig. 1. The schematic circuit design. The left part consists of a superconducting qubit (green) coupled to a readout resonator (yellow). The right part is a tunable lossy resonator (blue) containing a $\lambda/4$ resonator and a SQUID. The resonate frequencies of the qubit, readout resonator, lossy resonator are ω_q, ω_{r_1}, and ω_{r_2}, respectively. The waveguide at the bottom connects two resonators. The coupling strength between the resonators and waveguide is κ_n, $n = 1, 2$, respectively; $\kappa_1 \ll \kappa_2$. The distance between the two resonators is d. Inset: the readout resonator acts as the discrete 'dark' mode, and the lossy resonator acts as the continuum 'bright' mode. The interference between them will change the transmission spectra of the discrete one.

3. Interference between resonators

Inspired by the Purcell filter design, we investigate the waveguide-mediated interaction between distant resonators. We want to find a configuration that protects the qubit or resonator from decoherence. The Hamiltonian of this system is ($\hbar = 1$)

$$H_{\mathrm{sys}} = H_{\mathrm{JC}} + \omega_{r_2} a_2^\dagger a_2 + \sum_{n,m} \int \mathrm{d}\omega \omega b_n^{m\dagger}(\omega) b_n^m(\omega) + \sum_{n,m} \mathrm{i} \int \mathrm{d}\omega \kappa_n(\omega) \left[b_n^{m\dagger}(\omega) a_n - a_n^\dagger b_n^m(\omega) \right], \quad (2)$$

where the first term represents the JC Hamiltonian in Eq. (1), the second is the lossy resonator in blue, the third is the waveguide field modes, and the fourth describes the resonator–waveguide interaction. $a_n^\dagger$ (a_n) is the creation (annihilation) operator of the n-th resonator, ω_{r_n} is its resonant frequency. $b_n^{m\dagger}$ (b_n^m) is the creation (annihilation) operator of the photon towards right ($m = \mathrm{R}$) or left ($m = \mathrm{L}$). $\kappa_n(\omega)$ is the coupling strength between the resonator and the waveguide.

We neglect the qubit and explore the interference between the resonators. When this system works in the Markov regime, the equation of motion for the n-th resonator is[20–22]

$$\dot{a}_n = \left(-\mathrm{i}\omega_{r_n} a_n - \frac{\kappa_n}{2} a_n \right) - \sqrt{\frac{\kappa_n}{2}} \left(b_{n+}^{\mathrm{L}} + b_{n+}^{\mathrm{R}} \right). \quad (3)$$

where b_{n+}^{R} (b_{n+}^{L}) represent the input field of the n-th resonator which propagates to right (left). $b_{1+}^{\mathrm{R}}(t)$ and $b_{1+}^{\mathrm{R}\dagger}(t)$ are the quantum white noise operators, satisfying the commutation relations $[b_{1+}^{\mathrm{R}}(t), b_{1+}^{\mathrm{R}\dagger}(t)] = \delta(t - t')$.[23,24] The input–output fields through the resonators can be expressed as

$$b_{n-}^{\mathrm{L}} = b_{n+}^{\mathrm{L}} + \sqrt{\frac{\kappa_n}{2}} a_n, \quad b_{n-}^{\mathrm{R}} = b_{n+}^{\mathrm{R}} + \sqrt{\frac{\kappa_n}{2}} a_n. \quad (4)$$

The fields through the bottom waveguide are

$$b_{2+}^{\mathrm{R}} = \mathrm{e}^{\mathrm{i}\varphi} b_{1-}^{\mathrm{R}}, \qquad b_{1+}^{\mathrm{L}} = \mathrm{e}^{\mathrm{i}\varphi} b_{2-}^{\mathrm{L}}, \quad (5)$$

where $\varphi = k(\omega)d = \omega d/v$ is the phase difference arising from the resonator separation, $k(\omega)$ describes the dispersion relation of the waveguide, and v is the speed of the microwave in this device. Inserting Eqs. (4) and (5) to Eq. (3), we can obtain

$$\dot{a}_1 = \left(-\mathrm{i}\omega_{r_1} a_1 - \frac{\kappa_1}{2} a_1 \right) - V a_2 - \sqrt{\frac{\kappa_1}{2}} (b_{1+}^{\mathrm{R}} + \mathrm{e}^{\mathrm{i}\varphi} b_{2+}^{\mathrm{L}}), \quad (6)$$

$$\dot{a}_2 = \left(-\mathrm{i}\omega_{r_2} a_2 - \frac{\kappa_2}{2} a_2 \right) - V a_1 - \sqrt{\frac{\kappa_2}{2}} (b_{2+}^{\mathrm{L}} + \mathrm{e}^{\mathrm{i}\varphi} b_{1+}^{\mathrm{R}}), \quad (7)$$

where $V = \mathrm{e}^{\mathrm{i}\varphi} \sqrt{\kappa_1 \kappa_2/4}$ is the waveguide-mediated interaction parameter. Considering the field is coming from one side, $b_{2+}^{\mathrm{L}} = 0$, we can obtain the transmission amplitude by the transfer matrix as

$$T = \left| \frac{t_1 t_2}{\mathrm{e}^{-\mathrm{i}\varphi} - r_1 r_2 \mathrm{e}^{\mathrm{i}\varphi}} \right|^2, \quad (8)$$

where t_n and r_n are the transmission and reflection coefficients of the n-th resonator

$$t_n = \frac{\mathrm{i}\Delta_n(\omega)}{\mathrm{i}\Delta_n(\omega) + \kappa_n/2}, \quad r_n = -\frac{\kappa_n/2}{\mathrm{i}\Delta_n(\omega) + \kappa_n/2}, \quad (9)$$

where $\Delta_n(\omega) = \omega_{r_n} - \omega$ is the frequency detuning between the n-th resonator ω_{r_n} and the probe field ω.

When the frequency detuning between the resonators, $\delta_{r_2,r_1} = \omega_{r_2} - \omega_{r_1}$, is within the line width of the lossy one κ_2, the transmission amplitude in Eq. (8) with different d is shown in Fig. 2(a). The waveguide-mediated interaction arising from V can be real, imaginary, and complex. It determines the line shape symmetry of the readout resonator, as shown in Fig. 2(b). In experiments, we can fit the transmission curve by the Fano formula

$$F(\omega) = F_0 + H \frac{[q + 2(\omega - \omega_0)/\Gamma]^2}{1 + [2(\omega - \omega_0)/\Gamma]^2}, \quad (10)$$

where F_0 and H are constant factors, q determines the curve asymmetry, ω_0 is the discrete state frequency, and Γ is the resonance linewidth.[14,15] Here, we extend Fano's theory to our system, and the variation of the readout resonator line shape comes from the interference between a discrete state and a continuum state (see inset in Fig. 1).

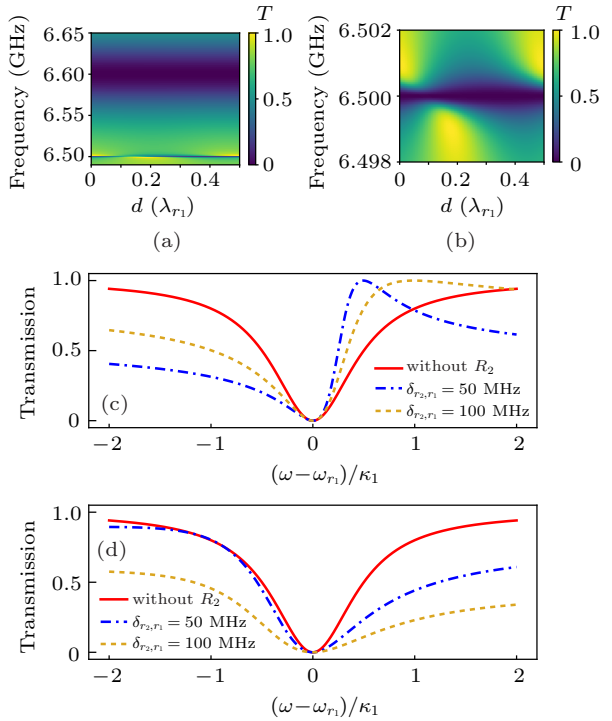


Fig. 2. (a) The transmission spectra of two resoantors with different separation distance d. $\omega_{r_2} = 6.6$ GHz. (b) Zoom image of the readout resonator at 6.5 GHz. (c) The transmission around the readout resonator with different δ_{r_2,r_1} and $d = 0$. (d) The transmission around the readout resonator with different δ_{r_2,r_1} and $d = 0.25\lambda_{r_1}$. The other parameters are $\omega_{r_1} = 6.5$ GHz, $\kappa_1 = 1$ MHz, $\kappa_2 = 100$ MHz, and $d = m\lambda_{r_1}$. Here λ_{r_1} is the wavelength corresponding to ω_{r_1}.

After the device fabrication, we can only control δ_{r_2,r_1} by the external magnetic field. In practice, we show the transmission spectrums as a function of δ_{r_2,r_1} with fixed d. For the case of $d = 0$ [see Fig. 2(c)], the lineshape of the readout resonator becomes asymmetric. It is getting sharper as δ_{r_2,r_1} decreases. The perfect transmission points $T \approx 1$ locate between the two resonant frequencies. For the case of $d = \lambda_{r_1}/4$ [see Fig. 2(d)], the readout resonator linewidth is getting broader, and there is no perfect transmission point.

4. Effective decay rate

From Eq. (10) and Fig. 2(b), we find that the line shape and bandwidth (decay rate) of the readout resonator Γ_{r_1} are related to the interference effect. In this section, we provide a theoretical analysis of Γ_{r_1}, as well as the effective decay rate of the qubit Γ_q.

The basis of our system is $|lmn\rangle$, where l, m, n correspond to the qubit, the readout resonator, and the lossy resonator, respectively. In the single-excitation subspace, the master equation of this system is $\dot{\rho} = -\mathrm{i}[H_{\mathrm{sys}}, \rho]$ and the evolution of the decaying wavefunction is $|\psi(t)\rangle = c_q(t)|e\rangle + c_{r_1}(t)|r_1\rangle + c_{r_2}(t)|r_2\rangle$, where $|e\rangle$, $|r_1\rangle$, and $|r_2\rangle$ represent the bare states $|e00\rangle$, $|010\rangle$, and $|001\rangle$, respectively. c_q, c_{r_1}, and c_{r_2} are the probability amplitudes of the qubit, the readout resoantor, and the lossy resonator

$$\dot{c}_q = -\mathrm{i}\omega_q c_q - \mathrm{i}g c_{r_1}, \tag{11}$$

$$\dot{c}_{r_1} = \left(-\mathrm{i}\omega_{r_1} c_{r_1} - \frac{\kappa_1}{2} c_{r_1}\right) - V c_{r_2} - \mathrm{i}g c_q, \tag{12}$$

$$\dot{c}_{r_2} = \left(-\mathrm{i}\omega_{r_2} c_{r_2} - \frac{\kappa_2}{2} c_{r_2}\right) - V c_{r_1}. \tag{13}$$

Since $\kappa_1 \ll \kappa_2$, the evolution of the lossy resonator is faster. We assume that it is in the steady state, $\dot{c}_{r_2} = 0$, then Eq. (13) can be expressed as

$$c_{r_2} = \frac{V}{-\mathrm{i}\omega_{r_2} - \kappa_2/2} c_{r_1}. \tag{14}$$

Insert Eq. (14) to Eq. (12) and ignore the qubit-resonator interaction term $-\mathrm{i}g_{c_q}$, we can obtain the new probability amplitudes of the readout resonator. The imaginary part represents the frequency shift arising from the waveguide-mediated interaction, and the real part decides the effective decay rate of the readout resonator. Under the rotating wave approximation, we arrive at

$$\Gamma_{r_1} = \kappa_1 - \frac{\kappa_1 \kappa_2 [\kappa_2 \cos(2\varphi)/2 + \delta_{r_2,r_1} \sin(2\varphi)]}{8\delta_{r_2,r_1}^2 + 2\kappa_2^2}. \tag{15}$$

According to the theory, one can protect an atom from decoherence by placing it in front of a mirror.[25,26] In our model, the lossy resonator acts as a frequency selective mirror, and the interference between resonators can change Γ_{r_1}, as shown in Fig. 3(a). The red region indicates $\Gamma_{r_1} > \kappa_1$, and the blue region is on the contrary $\Gamma_{r_1} < \kappa_1$. It differs from the direct resonator–resonator coupling system that Γ_{r_1} only relates to δ_{r_2,r_1}. When $\delta_{r_2,r_1} \to 0$, Γ_{r_1} comes to the perfect mirror case with $\Gamma_{r_1}^{\max} = 2\kappa_1$. We find that it is possible to suppress the readout resonator decay at finite frequency detuning. A similar method can be extended to the qubit–waveguide system.

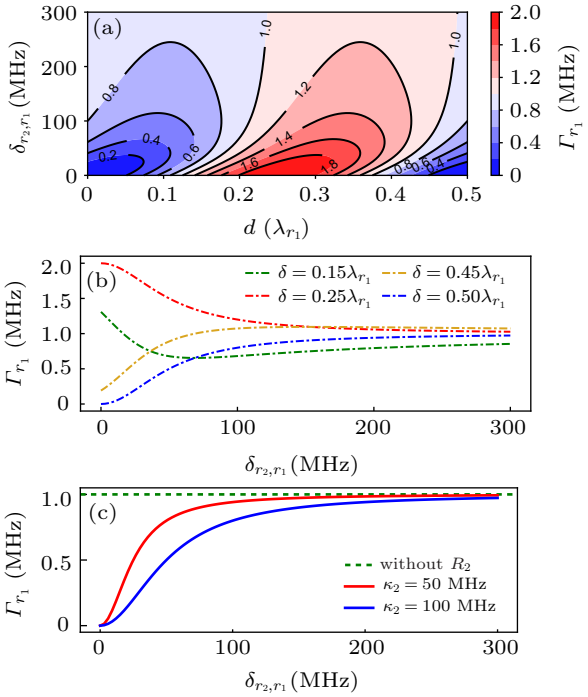


Fig. 3. (a) and (b) The effective decay rate of the readout resonator as a function of δ_{r_2,r_1} and $d = m\lambda_{r_1}$. Here λ_{r_1} is the wavelength corresponding to ω_{r_1}. $\kappa_2 = 100$ MHz. (c) The effective decay rate of the readout resonator with different κ_2 and δ_{r_2,r_1} at $d = 0$. The other parameters are $\kappa_1 = 1$ MHz and $\omega_{r_1} = 6.5$ GHz.

In practice, we can change ω_{r_2} by the external magnetic field, as shown in Fig. 3(b). Here Γ_{r_1} is a function of δ_{r_2,r_1} with fixed d, and this method has application in quantum storage. To reduce the inevitable fluctuations of d arising from the fabrication process, we can insert a SQUID to the readout resonator. Tuning ω_{r_1} and ω_{r_2} at the same time corresponds to changing the effective distance between the resonators.

In the following, we explore the impact of κ_2 on resonator decay suppression. Assuming $d = 0$, Γ_{r_1} with different κ_2 is shown in Fig. 3(c). When $\delta_{r_2,r_1} \neq 0$, we can increase κ_2 to reduce the effective decay rate of the readout resonator.

Now we further investigate the effective decay rate of the qubit. Aussuming $\dot{c}_{r_2} = 0$ in Eq. (13) and $\dot{c}_{r_1} = 0$ in Eq. (12), putting the results to $\dot{c}_q$ in Eq. (11), we can obtain the effective decay rate of the qubit as

$$\Gamma_q = \left| \mathrm{Re} \frac{2g^2}{-\mathrm{i}\delta_{r_1,q} - \kappa_1/2 - V^2/(-\mathrm{i}\delta_{r_2,q} - \kappa_2/2)} \right|, \quad (16)$$

where $\delta_{r_1,q} = \omega_{r_1} - \omega_q$ is the frequency detuning between the readout resonator and the qubit, and $\delta_{r_2,q} = \omega_{r_2} - \omega_q$ is the frequency detuning between the lossy resonator and the qubit.

Just like the interference between resonators, the effective decay rate of the qubit Γ_q is determined by $\delta_{r_2,q}$ and d, as shown in Fig. 4(a). The red region indicates $\Gamma_q > \gamma$, and the blue region is on the contrary $\Gamma_q < \gamma$, where γ is the qubit decay rate without the lossy resonator. In experiments, we can change ω_q and ω_{r_2} at the same time, and this corresponds to changing the effective distance between them. When $d = 0$ and $\delta_{r_1,q} \neq 0$, as shown in Fig. 4(b), a larger κ_2 corresponds to a better qubit decay suppression. Here the lossy resonator acts as a Purcell filter.

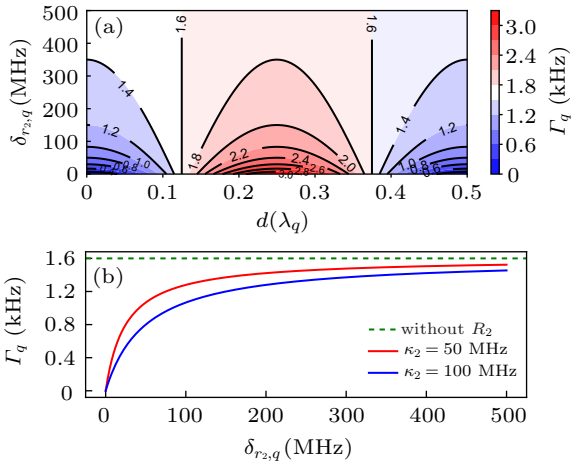


Fig. 4. (a) The effective decay rate of the qubit as a function of $\delta_{r_2,q}$ and $d = m\lambda_q$. Here λ_q is the wavelength corresponding to ω_q. $\kappa_2 = 100$ MHz. (b) The effective decay rate of the qubit with different κ_2 and $\delta_{r_2,q}$ at $d = 0$. The other parameters are $\kappa_1 = 1$ MHz, $g = 20$ MHz, $\omega_{r_1} = 6.5$ GHz, and $\omega_q = 6$ GHz. The qubit decay rate is $\gamma \approx \kappa_1 g^2/\delta_{r_1,q}^2 = 1.6$ kHz when the lossy resonator is absent.

5. Conclusion

In summary, we show the interference effect between distant resonators with different decay rates. The mirror-like lossy resonator provides a tunable boundary condition and can protect the readout one from decay. To improve the coherence time of qubits, we can switch off the decay channel by properly arranging the lossy resonator.

Looking forward, the asymmetric Fano lineshape has application in quantum sensing, and our approach can be extended to the qubit–waveguide system. This integrated circuit has the potential for the quantum information process and quantum control.

References

[1] Blais A, Huang R S, Wallraff A, Girvin S M and Schoelkopf R J 2004 *Phys. Rev. A* **69** 062320
[2] Stockklauser A, Scarlino P, Koski J V, Gasparinetti S, Andersen C K, Reichl C, Wegscheider W, Ihn T, Ensslin K and Wallraff A 2017 *Phys. Rev. X* **7** 011030
[3] Bianchetti R, Filipp S, Baur M, Fink J M, Göppl M, Leek P J, Steffen L, Blais A and Wallraff A 2009 *Phys. Rev. A* **80** 043840
[4] Yang D, Laflamme C, Vasilyev D V, Baranov M A and Zoller P 2018 *Phys. Rev. Lett.* **120** 133601
[5] Ritsch H, Domokos P, Brennecke F and Esslinger T 2013 *Rev. Mod. Phys.* **85** 553
[6] Bloembergen N, Purcell E M and Pound R V 1948 *Phys. Rev.* **73** 679
[7] O'Brien K, Macklin C, Siddiqi I and Zhang X 2014 *Phys. Rev. Lett.* **113** 157001
[8] Sete E A, Martinis J M and Korotkov A N 2015 *Phys. Rev. A* **92** 012325
[9] Reed M D, Johnson B R, Houck A A, DiCarlo L, Chow J M, Schuster D I, Frunzio L and Schoelkopf R J 2010 *Appl. Phys. Lett.* **96** 203110
[10] Sete E A, Gambetta J M and Korotkov A N 2014 *Phys. Rev. B* **89** 104516
[11] Yin Y, Chen Y, Sank D, O'Malley P J J, White T C, Barends R, Kelly J, Lucero E, Mariantoni M, Megrant A, Neill C, Vainsencher A, Wenner J, Korotkov A N, Cleland A N and Martinis J M 2013 *Phys. Rev. Lett.* **110** 107001
[12] Jeffrey E, Sank D, Mutus J Y, White T C, Kelly J, Barends R, Chen Y, Chen Z, Chiaro B, Dunsworth A, Megrant A, O'Malley P J J, Neill C, Roushan P, Vainsencher A, Wenner J, Cleland A N and Martinis J M 2014 *Phys. Rev. Lett.* **112** 190504
[13] Fleischhauer M, Imamoglu A and Marangos J P 2005 *Rev. Mod. Phys.* **77** 633
[14] Limonov M F, Rybin M V, Poddubny A N and Kivshar Y S 2017 *Nature Photonics* **11** 543
[15] Miroshnichenko A E, Flach S and Kivshar Y S 2010 *Rev. Mod. Phys.* **82** 2257
[16] Kannan B, Ruckriegel M J, Campbell D L, Kockum A F, Braumüller J, Kim D K, Kjaergaard M, Krantz P, Melville A, Niedzielski B M, Vepsäläinen A, Winik R, Yoder J L, Nori F, Orlando T P, Gustavsson S and Oliver W D 2020 *Nature* **583** 775
[17] Koch J, Yu T M, Gambetta J, Houck A A, Schuster D I, Majer J, Blais A, Devoret M H, Girvin S M and Schoelkopf R J 2007 *Phys. Rev. A* **76** 042319
[18] Schreier J A, Houck A A, Koch J, Schuster D I, Johnson B R, Chow J M, Gambetta J M, Majer J, Frunzio L, Devoret M H, Girvin S M and Schoelkopf R J 2008 *Phys. Rev. B* **77** 180502
[19] Bruce S W and Knight P L 1993 *J. Modern Optics* **40** 1195
[20] Xiao Y F, Li M, Liu Y C, Li Y, Sun X D and Gong Q H 2010 *Phys. Rev. A* **86** 065804
[21] Peng Z H, Jia C X, Zhang Y Q, Yuan J B and Kuang L M 2020 *Phys. Rev. A* **102** 043527
[22] Lalumière K, Sanders B C, van Loo A F, Fedorov A, Wallraff A and Blais A 2013 *Phys. Rev. A* **88** 043806
[23] Joshua C, Kerckhoff J and Sarovar M 2017 *Advances in Physics: X* **2** 784
[24] Clerk A A, Devoret M H, Girvin S M, Marquardt F and Schoelkopf R J 2010 *Rev. Mod. Phys.* **82** 1155
[25] Hoi I C, Kockum A F, Tornberg L, Pourkabirian A, Johansson G, Delsing P and Wilson C M 2015 *Nat. Phys.* **11** 1045
[26] Tufarelli T, Ciccarello F and Kim M S 2013 *Phys. Rev. A* **87** 013820